Lecture 3: Standing Waves, Chladni Figures, and Accelerator Cavities

3.1 Patterns produced by resonance

Not every visible pattern is a self-organized dissipative structure. A vibrating plate or resonant cavity often displays an eigenmode selected by its geometry, boundary conditions, and driving frequency. These systems provide a valuable contrast to convection and chemical patterns.

For a one-dimensional wave displacement $\psi(x,t)$,

$$\frac{\partial^2 \psi}{\partial t^2} = c^2 \frac{\partial^2 \psi}{\partial x^2}. \tag{1}$$

Assuming $\psi(x,t) = X(x)\cos(\omega t)$ gives $X'' + k^2 X = 0$ with $k = \omega/c$. Fixed ends require $X(0) = X(L) = 0$, so

$$X_n(x) = A_n \sin\left(\frac{n\pi x}{L}\right), \qquad f_n = \frac{nc}{2L}. \tag{2}$$

The standing-wave nodes are positions where $X_n = 0$.

3.2 Chladni figures

When a thin elastic plate vibrates at resonance, sand grains tend to accumulate near nodal regions where the motion is weak. The resulting Chladni figures reveal the plate's mode shapes.

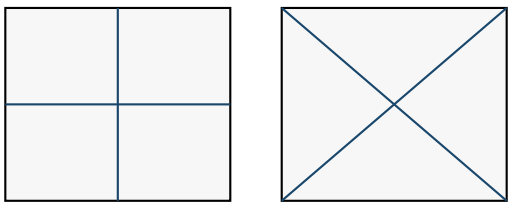


Figure 3. Simplified nodal-line sketches; actual patterns depend on the plate and its supports.

Unlike a stretched membrane, a thin bending plate is governed approximately by

$$D_b \nabla^4 w + \rho h \frac{\partial^2 w}{\partial t^2} = 0, \qquad D_b = \frac{E h^3}{12(1-\nu_p^2)}, \tag{3}$$

where h is plate thickness, E Young's modulus, ν_p Poisson's ratio, and D_b flexural rigidity. The fourth-order spatial derivative reflects bending resistance. The nodal geometry is highly sensitive to support conditions.

3.3 Electromagnetic standing waves

In an empty, source-free, perfectly conducting cavity, electromagnetic fields satisfy Maxwell's equations. Each Cartesian field component can be expressed in terms of spatial eigenfunctions satisfying a Helmholtz-type equation:

$$\nabla^2 \Psi + k^2 \Psi = 0, \qquad \omega = ck. \tag{4}$$

For an ideal rectangular cavity with side lengths a, b, d, the modal frequency has the form

$$f_{mnp} = \frac{c}{2}\sqrt{\left(\frac{m}{a}\right)^2 + \left(\frac{n}{b}\right)^2 + \left(\frac{p}{d}\right)^2}, \tag{5}$$

subject to the allowed TE/TM mode indices and boundary conditions.

3.4 Accelerator RF cavities

Charged-particle accelerators exploit resonant electromagnetic fields to transfer energy to a beam. The useful accelerating field is the longitudinal electric-field component E_z along the beam path. For a particle with charge q, the energy gain is

$$\Delta W = q \int_{\text{trajectory}} \mathbf{E} \cdot d\mathbf{l}, \tag{6}$$

evaluated along the particle's time-dependent trajectory. Synchronization between particle motion and RF phase is essential.

The quality factor

$$Q = \omega_0 \frac{U_{\text{stored}}}{P_{\text{lost}}} \tag{7}$$

measures how weakly a resonator dissipates stored energy. Real accelerator structures have complex geometries and mode spectra, and require electromagnetic design beyond the rectangular-cavity approximation.

3.5 Comparing mechanisms

Convection rolls require sustained thermal forcing and emerge through an instability. Chladni patterns and cavity fields are primarily *driven resonant eigenmodes*. Both show spatial order, but the physical selection mechanisms differ.

Key idea. Boundary conditions determine the allowed modes of a resonator. Mode selection is an important route to spatial structure, but it is not synonymous with spontaneous self-organization.

Further reading

L. D. Landau and E. M. Lifshitz, *Theory of Elasticity*; T. P. Wangler, *RF Linear Accelerators*.